6th AIAA Propulsion Aerodynamic Workshop 2023
Supersonic Axisymmetric Nozzles

July 1, 2022

Guidelines/Instructions for Participation in PAW06 Nozzle Test Case

Objectives

The main objective the 6th Propulsion Aerodynamics Workshop (PAW06) nozzle test case is to assess the accuracy of existing computational fluid dynamics (CFD) codes and modeling techniques in simulating the aerodynamics and thermodynamics of jet plumes from axisymmetric supersonic nozzles. Previous workshops focused on nozzle aerodynamics, propulsion efficiency, and heat transfer metrics. The PAW06 nozzle configurations under investigation will focus on experimental data from three supersonic axisymmetric nozzles, with different internal convergent-divergent (C-D) nozzle contours, each with same exit area, at a series of flow conditions where the jet pressure ratio (which prescribes a desired Mach number) and jet temperature were varied. Focus will be on predictions describing the plume development and plume turbulent statistics.

Background

Supersonic jet flow fields have been studied extensively over the years, with interest in understanding and predicting jet plume mixing for purposes of acoustics, plume thermal impacts, and mixing characteristics. One of the most extensively used databases for CFD validation was that collected by Seiner et al.[1] These experiments used total temperature and total pressure probes to measure the jets exhausting from axisymmetric Mach 2 nozzles at a series of temperatures. In Fig. 1, taken from Ref. 2, a typical result from applying standard Reynolds-averaged Navier-Stokes (RANS) two-equation turbulence modeling to a heated jet from the Seiner experiments is shown. It may be observed that the experimentally measured potential core length (or the region where the centerline velocity remains the same as the jet exit velocity) is nearly 10 nozzle diameters. Standard two-equation models with no corrections predict a potential core length that is substantially shorter than experimental data. However, utilizing the same RANS models with a correction for compressibility such as that of the well-known Sarkar[3] formulation produces a potential core longer than the experimentally observed values.

For reference, lower speed subsonic round jets, typically produce shorter potential core lengths. The data from Ref. 4 shows that the potential core length for an unheated round jet is approximately 5 nozzle diameters, and as the jet is heated the potential core slightly decreases in length. As the jet Mach number increases and approaches sonic exit velocity, experimental data generally shows that the potential core length increases, reaching approximately 7 nozzle diameters for an unheated jet. CFD using standard two-equation RANS turbulence modeling results in jet flow potential cores that are longer than the experimentally measured values for low Mach number jets (e.g. Ref. 5), in contrast to supersonic jets.

As a result, the general conclusion has been that uncorrected standard two-equation RANS models do not reproduce the experimentally observed reduction in mixing, which is believed to be due to compressibility. There have been several corrections proposed over the years in the same philosophy as

the Sarkar[3] formulation to predict the mixing in supersonic compressible jets more accurately, but to date these have been largely empirically based and do not enable a generalized improved capability that works for jet flows across a range in jet Mach number and jet temperature.

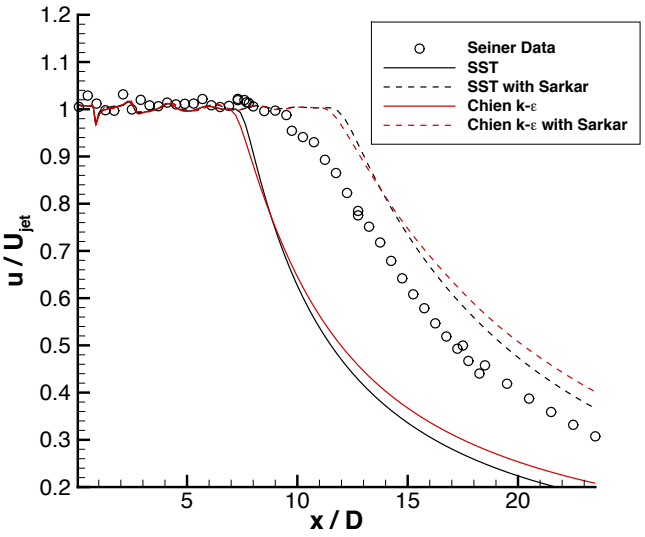

Figure 1.—RANS modeling for a heated Mach 2 round jet (taken from Ref. 2).

With the general deficiency of RANS-based CFD modeling for supersonic jets, application of large-eddy simulation (LES) has shown some promise for improved prediction of jet plumes from low speeds up to supersonic conditions. However, LES methods are substantially more computationally expensive, and applying an LES technique to both the jet plume region and the upstream wall bounded regions of the nozzle feeding the jet shear layer has been prohibitive. Hybrid RANS-LES and wall-modeled LES (WMLES) may offer promise for reducing the cost of the LES simulations, but without a resolved calculation of the boundary layers entering the jet shear layer, accurate prediction of the initial jet mixing region is potentially compromised.

In this workshop, the intention is to computationally investigate a series of supersonic jets, where the jet exit Mach number is varied. A relatively new experimental data set (Refs. 6-8), where detailed measurements of velocities and temperatures (including mean and RMS statistics) were obtained for axisymmetric supersonic jets with variation in jet exit Mach number and temperature, will be utilized in the computational studies. One of the nozzles used in the study, is a scaled version of the Mach 2 nozzle used in the studies of Seiner et al.[1] providing continuity to past validation efforts.

In this workshop, the degree of success of these simulations will be judged against measurements of velocities and temperatures, as well as turbulent statistics, in the jets issuing from three C-D nozzles. The velocities were measured using particle image velocimetry (PIV) and temperatures were measured using spontaneous rotational Raman scattering (SRS) spectroscopy.

Workshop Focus

The expected standard computational analysis technique is RANS. Application of standard one- or two-equation turbulence models as baseline results are acceptable to anchor participants' solutions

against expected results, but primary interest in RANS results submitted to this workshop are in advanced techniques such as Reynolds-stress models (RSMs) and explicit algebraic stress models (EASMs). Particular emphasis in this workshop will be on scale-resolving solutions (i.e. employing LES in the jet mixing region). Other novel methods are also of interest to the workshop, such as corrections to standard RANS models, as well as examination of newer grid methods such as adaptation.

Nozzle Configurations

The nozzles under consideration are all C-D nozzles tested at NASA Glenn Research Center (GRC) using the Small Hot Jet Acoustic Rig (SHJAR). A photograph of the end of this SHJAR with one of the C-D nozzles installed is shown in Fig. 1. The three C-D nozzles all had the same external geometric contour, and are attached to the nozzle adapter via set-screws. A cross-sectional view of the Mach 2.0 nozzle is shown in Fig. 2. The other two nozzles had design Mach numbers of 1.36 and 1.63. All of these three nozzles had the same exit diameter (50.8 mm), and the same internal length (165.1 mm) from the nozzle exit back to the junction with the nozzle adapter, with identical internal contour angle at this junction. As a result, only the internal contour from nozzle to nozzle differed, with different C-D nozzle throat location and diameter, but matching end points and angles. This facilitated the experimental setup and measurement procedures, and also facilitated computational grid generation for the meshes supplied for this workshop.

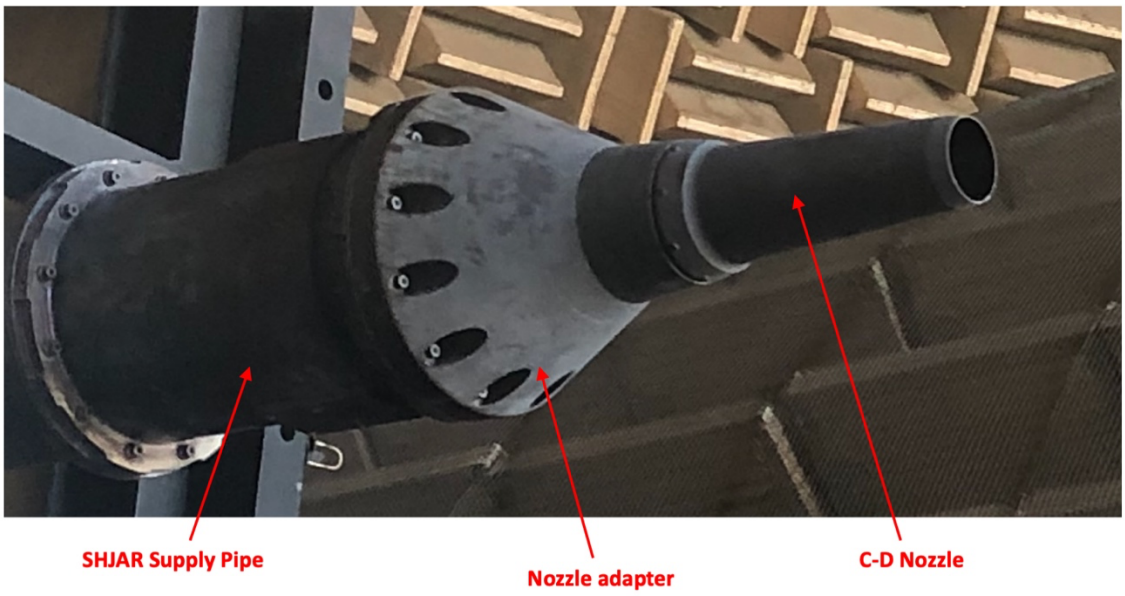

Figure 1.—Test rig (SHJAR) setup. All C-D nozzles have same exterior geometry.

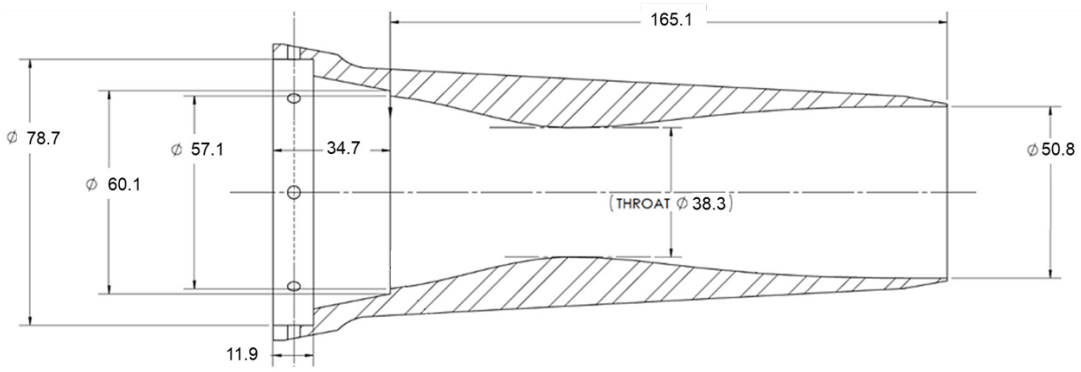

Figure 2.—Cross-section of Mach 2.00 axisymmetric nozzle (dimensions in mm)

The internal contours of all three nozzles were designed with the method of characteristics to provide as close to a uniform nozzle exit flow free of shock waves as possible. The Mach 2.00 nozzle has a divergent section (nozzle throat to exit) that has a geometrically scaled (reduced by a factor of 1.8) internal contour from the nozzle used by Seiner[1] et. al.

Flow Conditions and Nozzle Operation

Table 1 gives the five operating points that will be used as workshop test cases. References 6-8 describe 11 nozzle operating points that were investigated during the experimental program. For the workshop, we are requesting participants to focus on these five operating points.

Table 1. Operating Conditions

Case	Nozzle Geometry Mach No.	Nozzle Operating Mach No.	NPR	Nozzle Tt (K)	Jet ΔT (K) = $T_{s\text{-}jet} - T_{amb}$	$U_{jet\ (m/s)}$
1	1.36	1.36	3.01	715.2	233	622.9
2	1.63	1.63	4.44	799.4	233	746.6
3	2.00	2.00	7.82	939.7	233	916.0
4	1.63	1.36	3.01	715.2	233	622.9
5	1.63	1.63	4.44	442.1	0	555.2

In the experiments, the nozzle was operated by controlling the supply total pressure to achieve the jet exit Mach number (Mj) corresponding to a given nozzle pressure ratio (NPR = supply total pressure divided by ambient static pressure) and nozzle static temperature difference (ΔT = calculated jet exit static temperature - ambient static temperature). It is standard in many aerodynamic CFD simulations to assume a calorically perfect gas, such that the specific heat ratio, γ, is constant, and if the working fluid is air, γ = 1.4. The NPR and calculated jet Mach number, M_j, shown in Table 1 assumes γ = 1.4. For the calculations to be obtained for these workshop cases, this is an acceptable assumption, and

employing a variable γ capability is not expected to change the results significantly. In the test, hydrogen was combusted to heat the air to the desired temperature. For those interested in simulating gas properties other than air, please contact the committee and those conditions will be supplied. The primary effects of H_2O in the exhaust gas are to slightly reduce the nozzle flow rate and to marginally change the gas properties.

During the tests, the freestream conditions varied from day-to-day and even during a single day's testing, but for the purposes of CFD investigations, we recommend using a constant assumed static pressure of 99.28 kPA (14.4 psi) and static temperature of 288.9 K (520 R) for the ambient conditions. These reference ambient properties were used to calculate the ideal jet exit velocities shown in the table.

The first three cases shown in Table 1 represent variation in the jet exit Mach number, all at design NPRs for each respective nozzle geometry, and with jet exit ΔT = 233 K. The fourth case in the table examines an off-design, overexpanded case where the Mach 1.63 nozzle is run at a flow supply condition identical to that of the first case, which is on design for the Mach 1.36 nozzle. In other words, the NPR of this fourth case is too low to result in a fully expanded state at the nozzle exit for the Mach 1.63. The fifth case in the table is also for the Mach 1.63 nozzle, but uses an on-design pressure ratio and has ΔT = 0 K, or in other words no static temperature difference between the nozzle exhaust and the ambient air at the nozzle exit.

Computational Grids

A set of computational grids are being provided for workshop participants to use either exactly as provided or as a starting point for computational grids that they may prefer to use. These grids were constructed using the Pointwise software and used structured meshes for the axisymmetric geometry, that is - a planar cut of the geometry, with the axis of the nozzle and jet serving as the bottom of the grid. A view of the computational grid constructed for the Mach 2 nozzle is shown in Fig. 4. The internal geometry is reproduced exactly from that used in the experiment as far upstream as the supply pipe (see Fig. 1). The geometry of the outside of the nozzle, adapter, and supply pipe, is also modeled very closely with the exception that in this axisymmetric representation, the regions of the external surface locations where fasteners were used to attach the components of the assembly have been faired over. As the nozzle experiments were run with zero coflow, this change is not expected to be a significant modeling deviation. At the exit plane of the nozzle the lip thickness is 0.5 mm for all three nozzles.

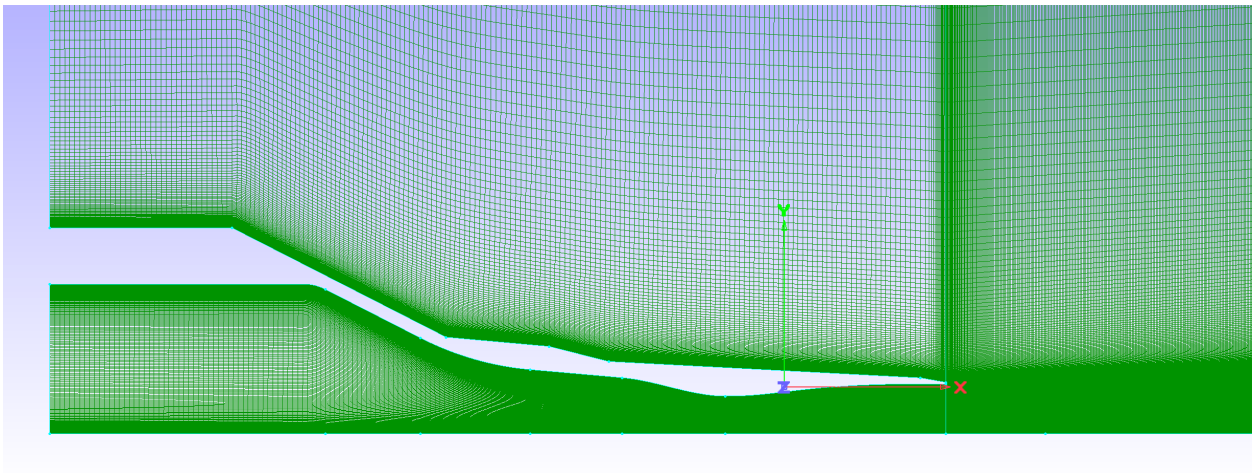

Figure 4.—Close-up of provided axisymmetric grid for the Mach 2 nozzle.

Using the structured grid approach, three zones were utilized with point-to-point matching at zonal interfaces. The location of the axis of symmetry at the nozzle exit is set as the origin of the computational domain (i.e. x,r = 0,0). Three zones comprised of: (1) nozzle internal region (401 axial points x 281 radial points for finest grid level), (2) external nozzle region and extending radially (201 x 161 points), (3) the jet plume region (961 x 481 points). These zones are point-to-point matched at zonal interfaces. The nozzle lip has 41 points. The axial spacing of the grid at the nozzle exit was 0.005 D, and the grids extended 40 D to the outflow boundary. Radially, the second zone has an inflow plane that extends 25 D away from the centerline. The farfield boundary has a 7.5 degree divergence angle, starting from zone 2 and extending into zone 3, to ensure that any ambient entrained air enters the flow domain. As a result, at the jet plume zone outflow station (at x/ D = 40) in zone 3, the farfield boundary extends to 32.45 D.

The structured grids, as supplied, may be coarsened in each computational direction such that grid convergence may be studied for RANS solvers. It is assumed that for scale-resolving methods, it may not be practical to study grid convergence and only one grid may be used based on solver requirements. These grids may be sequenced each direction 3 times to provide 4 grid sets with: (1) unsequenced: 401x281, 201x161, 961x481, (2) 1-level sequenced: 201x141, 101x81, 481x241, (3) 2-level sequenced: 101x71, 51x41, 241x121, (4) 3-level sequenced: 51x36, 26x21, 121x61.

While only the Mach 2 nozzle grid is shown here, the grids for the other two nozzles (Mach 1.36 and 1.63) are identical except for the last 165.1 mm of the nozzle (refer to Fig. 2) where the grids differ due to altered C-D contours in this region. The grids were packed such that the nominal y+ of the first point off the wall in the supersonic portion of the nozzle was on the order of 1. With only entrained slow flow outside the nozzle, the wall spacing on the external portion of the nozzle was packed much less tightly. Zones 2 and 3 are identical for the grids with each of the 3 C-D nozzles. Grid information is provided in the following format for each of the three nozzles: (1) Pointwise (3 structured zones) in units of inches (or normalized by nozzle exit radius = 1 in = 25.4 mm , (2) PLOT3D (3 structured zones) in units of meters, (3) internal nozzle surface contour in units of inches, also meters, (4) external nozzle surface in units of inches, also meters.

Note, these computational grids were built and checkout runs were conducted using CFD strategies very similar to the three test cases available via the NASA turbulence modeling resource

(turbmodels.larc.nasa.gov), namely the "Axisymmetric Subsonic jet," "Axisymmetric Hot Subsonic jet," and "Axisymmetric Near-sonic jet" cases. Visiting these validation pages and examining expected results may be instructive for workshop participants. The three-zone approach and overall gridding strategies were similar to the grids discussed here for the supersonic jet cases, although finer grid resolution in the potential core region was used here for the supersonic cases. There are two partially complete supersonic cases available on the website for two experimental points from the Seiner[1] experiments, but we recommend the grids and approaches supplied for this workshop.

Boundary Conditions and Flow Solver Settings

The boundary conditions required to run these nozzle cases are relatively straightforward, at least from a steady RANS solution approach. The stagnation pressure and temperature for each case may be obtained from Table 1 and applied at the inflow to the nozzle. In the experiments, there was no coflow, but some forward velocity needs to be prescribed with most CFD solvers to enable convergence. Preliminary test calculations were performed for the grids discussed in the previous section with multiple flow solvers utilizing a freestream condition set to Mach 0.01. It is desirable to set this freestream Mach number as low as possible but increasing it as high as Mach 0.05 should not affect the jet solutions significantly, if this is required to aid in solver convergence. On the finest grid level even with a steady RANS solver, participants may find that it is difficult to obtain a converged solution with a constant CFL solver approach. Experience has shown that completing these solutions with a time-accurate (constant time step) approach may be required to obtain a thoroughly converged RANS solution. As suggested in a previous section, we recommend using a constant assumed static pressure of 99.28 kPA (14.4 psi) and static temperature of 288.9 K (520 R) for the ambient conditions in these simulation cases.

It is believed that the flows inside the nozzles generated turbulent boundary layers, although measurements were not made inside the nozzle to verify this. Heat transfer to the nozzle structure is not expected to be a significant factor, so adiabatic wall boundary conditions may be set for the interior and exterior surfaces of the nozzle. The nozzle structure was constructed from 316 stainless steel for any participant wishing to calculate heat transfer to the structure. The default turbulent Prandtl number (Pr_t) used in most production CFD codes is 0.9 but there are some studies which have indicated that using $Pr_t = 0.7$ maybe more accurate for jet flows. Variable Pr_t approaches, if available to a participant, may be worthy of investigation.

Submission Data

- Information on the solver, RANS or LES. For RANS: solver name, turbulence model used, any corrections used, Pr_t, numerical scheme, inflow and wall boundary conditions, constant gamma or other special gas modeling. For LES: solver name, subgrid model, inflow and wall boundary conditions, details on whether WRLES, WMLES, hybrid RANS-LES, inflow treatment. *Note for RANS: Please verify the exact formulation of each turbulence model used, some codes have corrections hard-coded in that make them deviate from the true baseline model (see turbmodels.larc.nasa.gov)*
- Grid used – supplied (which level) or if custom: y+, total grid count, spacing details (such as Δx+, Δy+, Δz+, or other measure of grid size and stretching in the plume and in initial jet region.
- For RANS modeling, we are requesting solutions on the three finest level meshes. For scale-resolving simulations, it is recognized that these computations are very intensive and providing

solutions on multiple levels for every case may not be feasible, but it is still encouraged to provide solutions on at least two levels of grid refinement.

REQUIRED FLOW FIELD DATA:

- For scale-resolving: Number of "flow through periods" say in terms of (D/U_{jet}) and some indicator of "convergence" for scale resolving methods.
- Centerline velocity and temperature statistics data (in SI units of meters for lengths, m/s for velocities, K for tempratures - starting from nozzle exit to x/D = 20 (1.016 m): x, r, u, u', v', w', k, u'v', T, T'.
    - NOTES: (1) It is recognized that RANS codes may not yield statistics such as u', v', w', and T'. If this is the case, please still use the requested format but provide values of 0 in those columns. r-theta coordinates in 3D. (2) In the axisymmetric plane of the grid requested, $u = u_x$, $v = u_r$, $w = u_\theta$.
- Lipline (r = D/2) of the same quantities starting from nozzle exit to x/D = 20 (1.016 m).
- Radial profiles of the same quantities at stations: x/D=0,2,4,8,12,16 for radial positions from r/D =0 to r/D = 3 (0.1524 m). The exception is for X/D = 0 (nozzle exit), where radial positions from r/D =0 to r/D = 0.5 (0.0254 m) should be used. For this station, it may be best to use actual grid points if grid is packed to the nozzle surface, in order to characterize the boundary layer exiting the nozzle.
- Each data file should contain at least 200 points if equally spaced. Sample data files are provided with headers as requested.

References

1. Seiner, J. M., Ponton, M. K., Jansen, B. J., and Lagen, N. T., "The Effect of Temperature on Jet Noise Emission," AIAA Paper 92-02-046, 1992.
2. Georgiadis, N.J., Yoder, D.A., Vyas, M.A., and Engblom, W.A., "Status of Turbulence Modeling for Hypersonic Propulsion Flowpaths, ***Theor. Comput. Fluid Dyn***., Vol. 28, 2014, pp. 295-318.
3. Sarkar, S., Erlebacher, G., Hussaini, M.Y., Kreiss, H.O., "The Analysis and Modeling of Dilatational Terms in Compressible Turbulence," ***J. Fluid Mech.***, Vol. 227, 1991, pp.473–493.
4. Bridges, J. and Wernet, M. P., "Establishing Consensus Turbulence Statistics for Hot Subsonic Jets," AIAA Paper 2010-3751, June 2010.
5. Georgiadis, N.J., Yoder, D.A., and Engblom, W.A., "Evaluation of Modified Two-Equation Turbulence Models for Jet Flow Predictions, ***AIAA Journal***, Vol. 44, No. 12, Dec. 2006, pp. 3107-3114.
6. Georgiadis, N.J., Wernet, M.P., Locke, R.J., and Eck, D.G., "Mach Number and Heating Effects on Turbulent Supersonic Jets," AIAA Paper 2021-2834, Aug. 2021.
7. Wernet, M. P., Georgiadis, N. J., and Locke, R. J., "Velocity, Temperature and Density Measurements in Supersonic Jets," AIAA Paper 2021-0596, Jan. 2021.
8. Wernet, M. P., Georgiadis, N. J., and Locke, R. J., "Raman Temperature and Density Measurements in Supersonic Jets," ***Experiments. In Fluids***, Vol. 62, No. 3, 2021, pp. 1-21.